Human Radiation Dosimetry for the *N*-Methyl-D-Aspartate Receptor Radioligand ^{11}C-CNS5161

Vijay Dhawan[1], William Robeson[2], David Bjelke[1], Thomas Chaly[1], Kristin Graf[1], Matthew Hellman[1], Limei Zhuo[1], Meggan Mackay[3], and David Eidelberg[1]

[1]Center for Neurosciences, Feinstein Institute for Medical Research, Manhasset, New York; [2]Department of Radiology, North Shore–LIJ Health System, Manhasset, New York; and [3]Center for Autoimmune and Musculoskeletal Disease, Feinstein Institute for Medical Research, Manhasset, New York

^{11}C-CNS5161 (*N*-(2-chloro-5-methylthiophenyl)-*N*′-(3-methylthiophenyl)-*N*′-^{11}C-methylguanidine) has been successfully used in PET imaging of *N*-methyl-D-aspartate (NMDA) receptors. However, no human dosimetry data have been published. We are planning to use this radiotracer for investigating NMDA receptor function in systemic lupus erythematosus, traumatic brain injury, and Parkinson disease. We have therefore undertaken ^{11}C-CNS5161 PET imaging to measure the whole-body distribution of this radionuclide and to estimate radiation dose to various organs. **Methods:** Dynamic PET studies of the whole body were performed on 5 healthy adults. Regions of interest were drawn over the visualized structures. Resultant time–activity curves were generated and used to determine residence times for dosimetry calculations. S factors were implemented within the OLINDA/EXM software for each structure or organ. **Results:** For ^{11}C-CNS5161, organ doses ranged from 0.0002 to 0.0393 mGy/MBq (0.0006–0.1455 rad/mCi). The critical organ for radiation burden was the lungs, with a dose of 0.0393 mGy/MBq (0.1455 rad/mCi). Radiation doses to the reproductive and blood-forming organs were 0.0023, 0.0002, and 0.0020 mGy/MBq (0.0086, 0.0006, and 0.0074 rad/mCi) for the ovaries, testes, and red marrow, respectively. The effective dose equivalent was 0.0106 mSv/MBq (0.0392 rem/mCi). **Conclusion:** The radiation dosimetry for ^{11}C-CNS5161 for a standard single injection of 555 MBq (15 mCi) will result in an effective dose equivalent of 5.9 mSv (0.59 rem) and a lung dose of 21.8 mGy (2.18 rad) in young, healthy subjects.

Key Words: ^{11}C-CNS5161; dosimetry; PET

J Nucl Med 2015; 56:869–872
DOI: 10.2967/jnumed.114.152447

The *N*-methyl-D-aspartate (NMDA) receptor is a ligand-gated ion channel and mediates the effects of glutamate. Abnormalities of NMDA receptor function have been implicated in physiologic and pathologic processes, especially memory formation and excitotoxicity (*1*). Previous studies have also implicated NMDA receptor function in stroke, head injury, epilepsy, and Parkinson disease (*2*). Overexpression and phosphorylation of NMDA receptors have been demonstrated in dyskinesia after levodopa treatment in Parkinson disease (*3*). We are interested in investigating the role of the NMDA receptor in systemic lupus erythematosus (*4*), cognitive impairment after traumatic brain injury, and Parkinson disease.

^{11}C-CNS5161 (*N*-(2-chloro-5-methylthiophenyl)-*N*′-(3-methylthiophenyl)-*N*′-^{11}C-methylguanidine) is a selective noncompetitive antagonist of the NMDA glutamate receptor. Its synthesis was reported by Zhao et al. (*5*), and its use in vivo was reported by Schiffer et al. (*6*).

Even though a small number of PET studies using ^{11}C-CNS5161 have been published, no whole-body human dosimetry data are available. Similarly, other PET radiotracers are also under development for NMDA receptors, but human dosimetry data have not yet been published (*7,8*). We therefore undertook a whole-body PET imaging study of this radiotracer to obtain human dosimetry data.

MATERIALS AND METHODS

Five healthy control subjects were recruited (age range, 19–35 y; 3 men and 2 women; Table 1). The study was approved by the Institutional Review Board at North Shore University Hospital. Informed written consent was obtained from each subject after a detailed explanation of the study, which was conducted under Radioactive Drug Research Committee–approved protocols in which the dose limits are organ-based.

The radiotracer was synthesized using a minor modification of the published method of Zhao et al. (*5*). Briefly, the commercially avail-

TABLE 1
Demographics of the Healthy Volunteers

Subject no.	Sex	Age (y)	Height (cm)	Weight (kg)
1	M	22	198	95
2	M	31	170	84
3	M	35	198	84
4	F	19	160	51
5	F	23	168	65

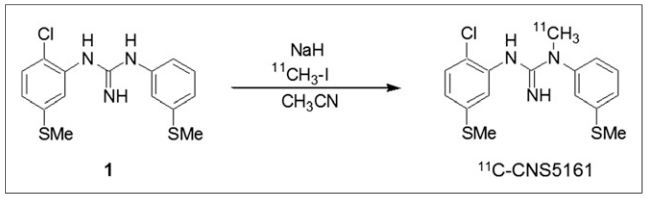

FIGURE 1. Radiosynthesis of ^{11}C-CNS5161.

Received Nov. 28, 2014; revision accepted Apr. 13, 2015.
For correspondence or reprints contact: Vijay Dhawan, Feinstein Institute for Medical Research, 350 Community Dr., Manhasset, NY 11030.
E-mail: dhawan@nshs.edu
Published online Apr. 30, 2015.

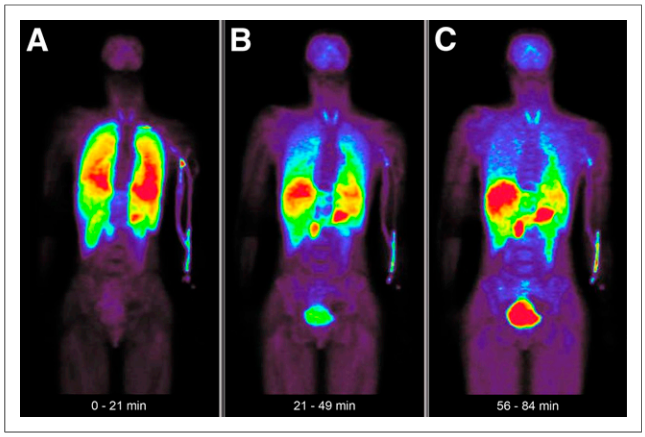

FIGURE 2. Early (A), mid (B), and late (C) ^{11}C-CNS5161 PET images of 26-y-old healthy woman. Uptake can be seen primarily in lungs in early image. By 30 min, decreasing uptake in lungs and increasing uptake in liver and gastrointestinal tract can be observed. In late image, increased uptake in liver, gastrointestinal tract, pancreas, bladder, and, to a lesser degree, thyroid and brain, is evident.

able desmethyl guanidine analog **1** was reacted with ^{11}C-methyl iodide in the presence of sodium hydride in acetonitrile (Fig. 1). Purification by semipreparative high-performance liquid chromatography afforded a clean separation of the product from other regioisomers. The product was then diluted in sterile water and purified further using a silica-based C18 Sep-Pak (Waters). Elution with ethanol and sterile saline yielded ^{11}C-CNS5161 with a radiochemical purity of at least 90% and a specific activity of at least 11 GBq/μmol (300 mCi/μmol).

Dynamic PET scans of the whole body were acquired in 2-dimensional mode on an Advance tomograph (GE Healthcare) with a 15-cm axial field of view. Two-dimensional mode imaging was used to avoid scatter from the bladder. For attenuation correction, transmission data using a ^{68}Ge rotating source were acquired before radiotracer injection. Approximately 555 MBq (15 mCi) of ^{11}C-CNS5161 were injected through a venous line in the arm. Dynamic imaging was initiated at the time of injection. The scanning protocol included 1-min emission scans for the first 4 cycles (each cycle is 7 bed positions) and 2 min for the next 4 cycles, covering the skull to mid thigh. The full-body scanning time was therefore 7 or 14 min, resulting in a total duration of 84 min (28 min for the first 4 cycles and 56 min for the next 4 cycles). Images were reconstructed in 2-dimensional mode using a manufacturer-supplied reconstruction technique (ordered-subsets expectation maximization with 16 subsets and 4 iterations).

Coronal images were reconstructed from the transaxial image set and then summed to create a composite image. Volumes of interest were drawn over the entire body and each visualized organ. Counts per voxel were multiplied by organ voxels to obtain total counts in each organ. Data were then normalized to the total body to compute specific organ uptake (this makes the calculations independent of organ mass). Time–activity curves for the organs were fit to a nonlinear regression model of exponential uptake and clearance, and analytic integration was used to estimate the area under the curve (AUC). Units for AUC are hours. A remainder term was computed for activity in the body not specifically visualized in an organ. Residence times were input to the OLINDA/EXM software for each organ based on the adult model to compute the organ doses and effective dose equivalent (*9*). This software multiplies residence time for each subject and organ by the S value (mSv/MBq × h) as follows:

$$\text{Dose}(\text{mSv}/\text{MBq}) = \text{residence time (h)} \times \text{S value}. \qquad \text{Eq. 1}$$

S values are implemented within the OLINDA/EXM software.

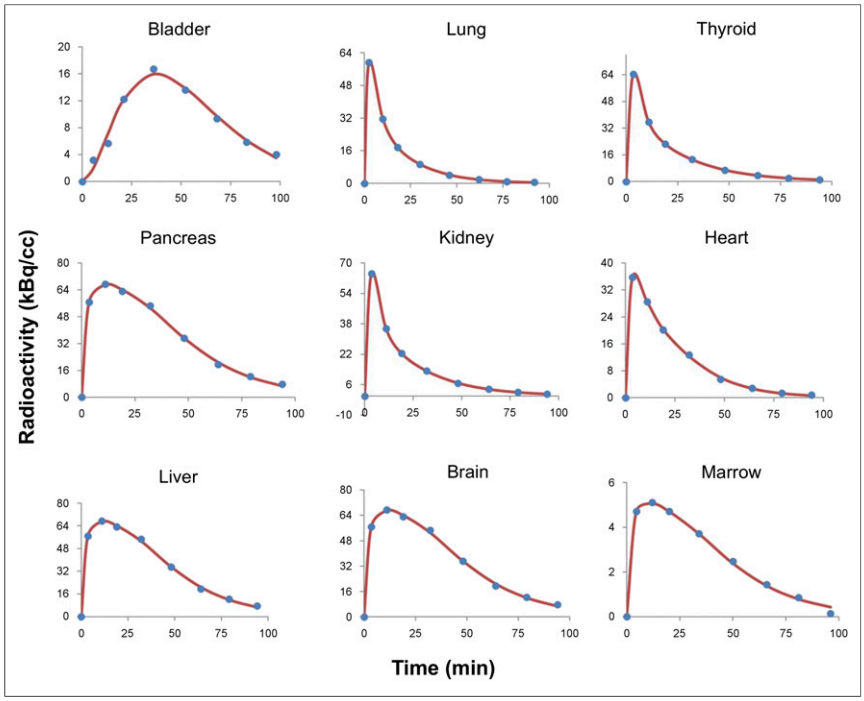

FIGURE 3. Typical time–activity curves from 9 sampled organs. *y*-axis scales vary for different organs. These curves were fitted using either sum of 2 exponentials or pulse function ($t \times e^{-kt}$) plus sum of 2 exponentials. AUCs were calculated and used for estimating absorbed dose to organ. Both maximum height and shape of curves determine AUCs, as is reflected in absorbed dose. t = time; e^{-kt} = exponential function with rate constant k.

RESULTS

Body images from a representative subject are presented in Figure 2. Each panel is a composite of 7 frames of 2-min duration each. The data were acquired in 2-dimensional mode to avoid scatter effects from the bladder. The figure shows composite images from 3 phases of the study: 0–21 min (early), 21–49 min (mid), and 56–84 min (late) after injection. Rapid uptake of radiotracer in the lungs was followed by a gradual decrease over the study duration; uptake in the liver, gastrointestinal tract, and pancreas increased continuously over 90 min; the bladder showed significant uptake toward the end because of urine accumulation.

Typical time–activity curves from the sampled organs are shown in Figure 3. The organs that followed a fast wash-in and washout were the lungs, kidneys, heart, and thyroid. The brain, marrow, pancreas, and liver demonstrated fast wash-in but a slower washout. Bladder activity showed a slow wash-in (gradual accumulation of urine radioactivity) and a slow washout.

TABLE 2
Dosimetry for ^{11}C-CNS5161

Parameter/organ	Dose		CV (%)
	mGy/MBq	rad/mCi	
Effective dose equivalent	0.0106*	0.0392†	13
Red marrow	0.0020	0.0074	3
Testes	0.0002	0.0006	15
Ovaries	0.0023	0.0086	3
Brain	0.0064	0.0238	12
Lungs	0.0393	0.1455	20
Heart	0.0034	0.0126	4
Liver	0.0061	0.0225	13
Spleen	0.0258	0.0953	43
Kidneys	0.0204	0.0755	33
Bladder	0.0075	0.0276	13
Stomach	0.0043	0.0161	43
Small intestine	0.0021	0.0078	6
Upper large intestine	0.0060	0.0222	44
Lower large intestine	0.0018	0.0065	11
Gallbladder wall	0.0027	0.0101	6
Thyroid	0.0221	0.0819	37

*mSv/MBq.
†rem/mCi.
CV = coefficient of variation: SD/mean.

These curves were fitted using a sum of rising and decaying exponentials. AUCs were calculated and used for estimating the absorbed dose to the organs.

Table 2 presents the results for 16 organs and the effective dose equivalent for the 5 subjects.

DISCUSSION

These dosimetry data show that—in order not to exceed a 50-mGy (5-rad) dose to the critical organ (lungs)—the maximum injected dose in ^{11}C-CNS5161 studies is 1,258 MBq (34 mCi). For two other ^{11}C-labeled radiotracers in common use, raclopride and Pittsburgh compound B, the estimated maximum dose is 1,591 and 1,184 MBq (43 and 32 mCi), respectively (*10–12*). However, it has been previously demonstrated that even with an injected dose of 555 MBq (15 mCi) for these radiotracers, images of acceptable quality have been acquired and quantitatively analyzed (*13,14*).

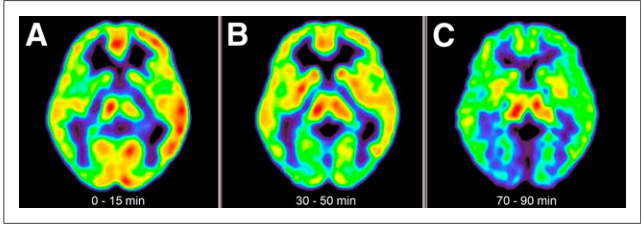

FIGURE 4. Early (A), mid (B), and late (C) ^{11}C-CNS5161 PET brain images of 34-y-old woman with systemic lupus erythematosus. Images were obtained using GE Advance tomograph (GE Healthcare) in 3-dimensional mode. Early blood-flow–like image changes to selective-regional-retention–like image by 90 min.

No animal dosimetry data have been published. However, data from biodistribution studies in rats are available (*1*). We have compared the AUCs derived from time–activity curves of percentage injected dose per organ with our human dose estimates. According to the AUCs, the relative uptake in rats follows this order: liver > lungs > kidneys > spleen > brain > heart. In our human study, the relative uptake followed this order: lungs > spleen > thyroid > kidneys > bladder > brain > liver. Thus, the distribution of this radiotracer in rats and humans is similar, except for the liver. Differences in the species and the study design could account for this observation. Effective dose equivalent and all organ dose levels were within radiation safety guidelines for injections of 555 MBq (15 mCi) (Table 2). For most ^{11}C radiotracers, the bladder does not seem to be a critical organ, unlike the case for various ^{18}F tracers such as ^{18}F-FDOPA (6-^{18}F-fluoro-L-dopa) and ^{18}F-FP-CIT (^{18}F-fluoropropyl-carbomethoxyiodophenylnortropane) (*15,16*).

To illustrate brain uptake at different times during a dynamic ^{11}C-CNS5161 PET study, in Figure 4 we present a scan of a 34-y-old woman with systemic lupus erythematosus (dedicated 3-dimensional brain imaging not used for dosimetry purposes). These typical brain images demonstrate the high quality of the images that can be acquired with a 555-MBq (15-mCi) bolus injection over a dynamic 90-min scan. The early phase shows a blood-flow–like image with cortical and subcortical uptake as expected. In the mid phase, radiotracer uptake starts to increase in the basal ganglia and thalamus. In the late phase, cortical uptake decreases whereas the thalamus and, to a lesser degree, the lentiform nuclei show significant uptake. This study suggests that multiple scans for different states or conditions can successfully be performed with an injected dose in the 370- to 555-MBq (10–15 mCi) range.

CONCLUSION

From the 5 subjects studied, the lungs appear to be the critical organ in ^{11}C-CNS5161 dosimetric considerations. The effective dose equivalent was 0.0106 mSv/MBq (0.0392 rad/mCi), which should easily allow for injections of 370–555 MBq (10–15 mCi) for PET studies using this radiotracer.

DISCLOSURE

The costs of publication of this article were defrayed in part by the payment of page charges. Therefore, and solely to indicate this fact, this article is hereby marked “advertisement” in accordance with 18 USC section 1734. This research was supported by the National Institutes of Health (grant 1P01AI073693-05) and the Lupus Foundation of America (grant 113121). David Eidelberg serves on the scientific advisory board and has received honoraria from the Michael J. Fox Foundation for Parkinson’s Research; is listed as coinventor of patents regarding markers for use in screening patients for nervous system dysfunction and a method and apparatus for using the same (without financial gain); and has received research support from the NIH (NINDS, NIDCD, and NIAID) and the Dana Foundation. No other potential conflict of interest relevant to this article was reported.

ACKNOWLEDGMENTS

We acknowledge Claude Margouleff for technical assistance with the PET studies and Yoon Young Choi for preparation of the manuscript.

REFERENCES

1. Biegon A, Gibbs A, Alvarado M, Ono M, Taylor S. In vitro and in vivo characterization of [^{3}H]CNS-5161—a use-dependent ligand for the N-methyl-D-aspartate receptor in rat brain. *Synapse.* 2007;61:577–586.
2. Benarroch EE. NMDA receptors: recent insights and clinical correlations. *Neurology.* 2011;76:1750–1757.
3. Ahmed I, Bose SK, Pavese N, et al. Glutamate NMDA receptor dysregulation in Parkinson's disease with dyskinesias. *Brain.* 2011;134:979–986.
4. Kowal C, Degiorgio LA, Lee JY, et al. Human lupus autoantibodies against NMDA receptors mediate cognitive impairment. *Proc Natl Acad Sci USA.* 2006;103: 19854–19859.
5. Zhao Y, Robins E, Turton D, Brady F, Luthra SK, Årstad E. Synthesis and characterization of N-(2-chloro-5-methylthiophenyl)-N′-(3-methylthiophenyl)-N′-[^{11}C]methylguanidine [^{11}C]CNS 5161, a candidate PET tracer for functional imaging of NMDA receptors. *J Labelled Comp Radiopharm.* 2006;49:163–170.
6. Schiffer WK, Pareto-Onghena D, Wu H, et al. In vivo evaluation of [^{11}C]CNS-5161 as a use-dependent ligand for the NMDA glutamate receptor channel [abstract]. *J Cereb Blood Flow Metab.* 2005;25(suppl):S595.
7. Kumlien E, Hartvig P, Valind S, Oye I, Tedroff J, Langstrom B. NMDA-receptor activity visualized with (S)-[N-methyl-^{11}C]ketamine and positron emission tomography in patients with medial temporal lobe epilepsy. *Epilepsia.* 1999;40: 30–37.
8. McGinnity CJ, Hammers A, Riano Barros DA, et al. Initial evaluation of ^{18}F-GE-179, a putative PET tracer for activated N-methyl D-aspartate receptors. *J Nucl Med.* 2014;55:423–430.
9. Stabin MG, Sparks RB, Crowe E. OLINDA/EXM: the second-generation personal computer software for internal dose assessment in nuclear medicine. *J Nucl Med.* 2005;46:1023–1027.
10. Scheinin NM, Tolvanen TK, Wilson IA, Arponen EM, Nagren KA, Rinne JO. Biodistribution and radiation dosimetry of the amyloid imaging agent ^{11}C-PIB in humans. *J Nucl Med.* 2007;48:128–133.
11. Slifstein M, Hwang DR, Martinez D, et al. Biodistribution and radiation dosimetry of the dopamine D2 ligand ^{11}C-raclopride determined from human whole-body PET. *J Nucl Med.* 2006;47:313–319.
12. van der Aart J, Hallett WA, Rabiner EA, Passchier J, Comley RA. Radiation dose estimates for carbon-11-labelled PET tracers. *Nucl Med Biol.* 2012;39:305–314.
13. Brooks DJ, Ibanez V, Sawle GV, et al. Striatal D2 receptor status in patients with Parkinson's disease, striatonigral degeneration, and progressive supranuclear palsy, measured with ^{11}C-raclopride and positron emission tomography. *Ann Neurol.* 1992;31:184–192.
14. Klunk WE, Engler H, Nordberg A, et al. Imaging brain amyloid in Alzheimer's disease with Pittsburgh compound-B. *Ann Neurol.* 2004;55:306–319.
15. Dhawan V, Belakhlef A, Robeson W, et al. Bladder wall radiation dose in humans from fluorine-18-FDOPA. *J Nucl Med.* 1996;37:1850–1852.
16. Robeson W, Dhawan V, Belakhlef A, et al. Dosimetry of the dopamine transporter radioligand ^{18}F-FPCIT in human subjects. *J Nucl Med.* 2003;44:961–966.